MAJOR ARTICLE

Mechanisms Underlying Coagulation Abnormalities in Ebola Hemorrhagic Fever: Overexpression of Tissue Factor in Primate Monocytes/Macrophages Is a Key Event

Thomas W. Geisbert,[1] Howard A. Young,[3] Peter B. Jahrling,[2] Kelly J. Davis,[2] Elliott Kagan,[4] and Lisa E. Hensley[1]

[1]Virology Division and [2]Headquarters, United States Army Medical Research Institute of Infectious Diseases, Fort Detrick, [3]Cellular and Molecular Immunology Section, Laboratory of Experimental Immunology, National Cancer Institute, Frederick Cancer Research and Development Center, Frederick, and [4]Department of Pathology, Uniformed Services University of the Health Sciences, Bethesda, Maryland

Disseminated intravascular coagulation is a prominent manifestation of Ebola virus (EBOV) infection. Here, we report that tissue factor (TF) plays an important role in triggering the hemorrhagic complications that characterize EBOV infections. Analysis of samples obtained from 25 macaques showed increased levels of TF associated with lymphoid macrophages, whereas analysis of peripheral blood–cell RNA showed increased levels of TF transcripts by day 3. Plasma from macaques contained increased numbers of TF-expressing membrane microparticles. Dysregulation of the fibrinolytic system developed during the course of infection, including a rapid decrease in plasma levels of protein C. Infection of primary human monocytes/macrophages (PHMs) was used to further evaluate the role of TF in EBOV infections. Analysis of PHM RNA at 1–48 h showed increased TF transcripts, whereas levels of TF protein were dramatically increased by day 2. Thus, chemotherapeutic strategies aimed at controlling overexpression of TF may ameliorate the effects of EBOV hemorrhagic fever.

Among viruses that cause hemorrhagic fever (HF), Ebola virus (EBOV) stands out for its impressive lethality. Along with Marburg virus, the 4 species of EBOV (Zaire, Sudan, Reston, and Ivory Coast) make up the negative-stranded, enveloped RNA virus family *Filoviridae*. In outbreaks among humans, acute mortality caused by the Zaire species of EBOV has been ~80% [1]; in monkey models of the genus *Macaca*, acute mortality caused by the Zaire species of EBOV has been >90% [2–4]. As with septic shock caused by bacterial pathogens, the fulminant end of the spectrum of disease triggered by EBOV infection is thought to involve inappropriate or maladaptive host responses. The parallels of EBOV HF with septic shock are instructive. Among processes, mediators, and pathways thought to be dysregulated in both EBOV HF and septic shock are lymphocyte apoptosis (i.e., massive apoptosis of lymphocytes both intravascularly and in lymphoid organs), proinflammatory cytokines, and the coagulation cascade (i.e., disseminated intravascular coagulation [DIC]).

DIC is neither a disease nor a symptom; rather, it is a syndrome characterized by activation of the coagulation system, either in a localized region or throughout the entire vascular system, leading to histologically visible microthrombi generated in the microvasculature [5–7]. These microthrombi may hamper adequate blood supply, thereby contributing to the multiple organ dysfunction and high mortality characteristic of EBOV infection. In fact, there is ample experimental and pathological evidence that fibrin deposition contributes to multiple organ failure [8, 9]. Before acute

Received 12 February 2003; accepted 9 June 2003; electronically published 14 November 2003.

Presented in part: XII International Congress of Virology, Paris, 27 July–1 August 2002 (symposium V-293).

The views, opinions, and findings contained herein are those of the authors and should not be construed as an official Department of the Army position, policy, or decision unless so designated by other documentation.

Reprints or correspondence: Dr. Thomas W. Geisbert, USAMRIID, Attn: MCMR-UIV, 1425 Porter St., Fort Detrick, MD 21702-5011 (tom.geisbert@amedd.army.mil).

The Journal of Infectious Diseases 2003;188:1618–29

0022-1899/2003/18811-0002

DIC can become apparent, there must be sufficient stimulus to deplete or overwhelm the natural anticoagulant systems, such as the protein C system. During activation of the clotting system, the host will make an effort to block the process through inhibitors of the clotting system. In this process, however, the inhibitors are consumed, and, if the rate of consumption exceeds the rate of synthesis by liver parenchymal cells, plasma levels of inhibitors will decline. A number of studies have found positive correlations between plasma levels of inhibitors and the degree of DIC [6, 10].

During DIC, the extrinsic tissue factor (TF)–dependent pathway is the dominant route to thrombin generation that leads to fibrin deposition [6, 11]. Overexpresssion of TF, a 47-kDa transmembrane glycoprotein that functions as the primary cellular initiator of the coagulation protease cascades, is a leading cause of DIC and thrombosis-related organ failure [12]. In many cases, TF exposed to the circulation is the sole culprit underlying the initiation of DIC. Although endothelial cells can express large amounts of TF in vitro, most studies suggest that this is an artificial observation that is not relevant to in vivo settings. In contrast, synthesis and exposure of endothelial TF is very limited and not likely significant in emerging and ongoing DIC [13, 14]. Monocytic expression of TF can promote widespread clot formation in other diseases [14, 15]. Furthermore, increased levels of TF mRNA have been shown in mononuclear, but not endothelial, cells in lipopolysaccharide-treated rats [12, 16].

Although DIC is often viewed as a prominent manifestation of EBOV infection in primates, the presence of DIC in human filoviral infections has been a controversial topic; cultural mores and logistical problems have hampered systematic studies. No single laboratory test is sufficient to permit a definitive diagnosis of DIC; however, a positive D-dimer test is particularly useful in supporting a diagnosis of DIC because it indicates activation of both the clotting and fibrinolytic systems and because elevated levels of D-dimers are found in ~95% of all cases of DIC [6]. In most instances, a diagnosis of DIC can be made by taking into consideration the underlying disease in conjunction with a combination of laboratory findings [5–7]. With regard to human cases of filoviral infection, fibrin deposition has been documented at autopsy [17–19]; furthermore, clinical laboratory data suggest that DIC is likely to be a prominent feature of human disease [20–23]. We have a clearer picture of coagulation in nonhuman primates. Numerous studies have shown histological and biochemical evidence of DIC syndrome during EBOV infection in a variety of nonhuman primate species [2–4, 24–27]. However, with few exceptions, these investigations examined monkeys killed when moribund and shed little light on the pathogenesis of EBOV infection during the period before death. Despite progress made during the last decade to identify key modulators of EBOV pathogenesis, there is no universal concept of the triggering mechanism of the hemorrhagic diathesis of EBOV infection.

The aim of the present study was to investigate the processes that trigger the coagulation abnormalities that are characteristic of both human and nonhuman primate EBOV infections and to identify key targets for potential chemotherapeutic interventions. The in vivo portion of this study focused on longitudinal evaluation of various coagulation parameters in nonhuman primates that were experimentally infected with EBOV. In addition, we inoculated primary human monocytes/macrophages (PHMs), to further evaluate the potential triggers for DIC, including expression of TF.

MATERIALS AND METHODS

Animals and inoculations. Twenty-one healthy, filovirus-seronegative, adult male cynomolgus macaques *(Macaca fascicularis)* and 4 rhesus macaques *(Macaca mulatta)* were used for this study. Macaques were inoculated intramuscularly with 1 mL of virus stock that contained 1000 pfu of EBOV (Zaire 1995 strain) that had been isolated from the serum of a human patient in 1995 and had been passaged 3 times in Vero cells [28]. Scheduled necropsies were performed at days 1 (3 cynomolgus macaques), 2 (3 cynomolgus macaques), 3 (1 rhesus and 4 cynomolgus macaques), 4 (1 rhesus and 4 cynomolgus macaques), 5 (1 rhesus and 4 cynomolgus macaques), 6 (3 cynomolgus macaques), and 9 (1 rhesus macaque) after infection. Longitudinal blood samples were analyzed by coagulation assays, as described below. Rhesus macaques were not used for any temporal comparisons; rather, this small cohort of macaques was used to detect any clear species-specific differences among the macaques that may warrant additional studies, while conserving primate resources.

Ethical considerations. In conducting this research, we adhered to the Institute of Laboratory Animal Resources, National Research Council's *Guide for the Care and Use of Laboratory Animals*. Our animal facilities are fully accredited by the Association for Assessment and Accreditation of Laboratory Animal Care International. Human leukocytes used in this study were obtained from healthy donors, after receiving informed consent. These cells were obtained in accordance with a protocol (FY99-21) approved by the US Army Medical Research Institute of Infectious Diseases Office of Human Use and Ethics.

Cell cultures and viruses. Elutriated monocytes were obtained from healthy human donors, isolated according to conventional procedures, and cultured or differentiated in 6-well plates [29]. Normal primary human umbilical vein endothelial cells (HUVECs), pooled from several donors, and primary human lung-derived microvascular endothelial cells (HMVEC-Ls) were obtained from Clonetics and were maintained according

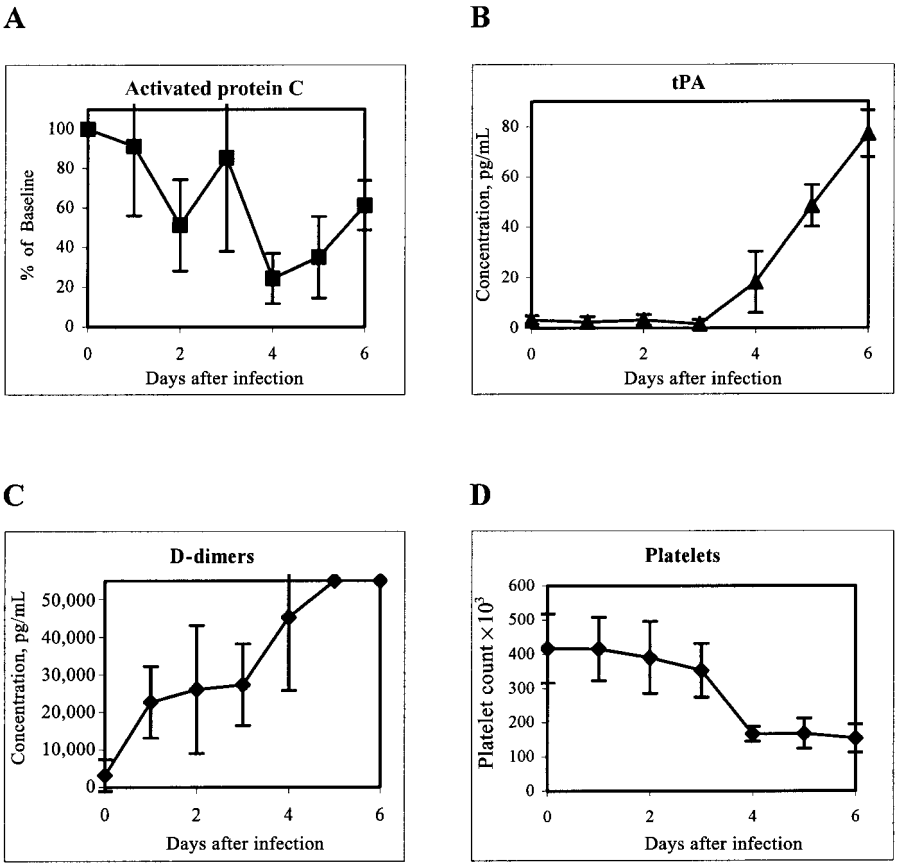

Figure 1. Development of coagulation abnormalities during Ebola virus (EBOV) infection of cynomolgus macaques. *A,* Plasma levels of activated protein C measured by a chromatic hydrolysis assay at days 1–6 after infection. *B,* Plasma levels of tissue-type plasminogen activator antigen (tPA) determined by ELISA at days 1–6. *C,* Plasma levels of D-dimers measured by ELISA at days 1–6. *D,* Development of thrombocytopenia. *A–C,* $n = 4$ at days 1–5 after infection, and $n = 3$ at day 6. *D,* $n = 12$ at days 1 and 2 after infection, $n = 10$ at day 3, $n = 7$ at day 4, and $n = 4$ at days 5 and 6.

to the supplier's recommendations. HUVECs and HMVEC-Ls were used at the second and third passages, respectively. Cultures were challenged with EBOV (Zaire 1995 strain) [28] at an MOI of 1.0. Culture medium from Vero cells represented a "virus-free stock" in all mock-infection experiments. Total RNA was extracted from infected/treated cells by use of Trizol (Life Technologies). Titration for infectious EBOV was determined as described elsewhere [3].

Coagulation tests. Plasma levels of D-dimers were measured by an ELISA, according to the manufacturer's directions (Diagnostica Stago). Plasma levels of protein C were determined by a chromatic hydrolysis assay (DiaPharma), according to the manufacturer's recommendations. To control background for nonspecific hydrolysis, sterile water was substituted for the protein C activator. Plasma levels of tissue-type plasminogen activator antigen (tPA), urokinase-type plasminogen activator (uPA), and factor VIIa (FVIIa) were determined by ELISA (American Diagnostica), according to the manufacturer's instructions.

Histopathology. Tissues were collected and immersion-fixed in 10% neutral-buffered formalin and processed for histopathology, immunohistochemistry, and transmission electron microscopy (TEM), as described elsewhere [3, 4]. Replicate sections of spleen, liver, and axillary lymph nodes were stained with phosphotungstic acid hematoxylin (PTAH), to demonstrate polymerized fibrin [4].

TEM of tissues. Paraformaldehyde/glutaraldehyde-fixed tissues and peripheral blood mononuclear cells (PBMCs) for TEM were postfixed in 1% osmium tetroxide in 0.1 mol/L phosphate buffer, rinsed, stained with 0.5% uranyl acetate in ethanol, dehydrated in graded ethanol and propylene oxide, and embedded in Poly/Bed 812 resin (Polysciences). Ultrathin sections were cut, placed on 300-mesh nickel TEM grids, and stained with uranyl acetate and lead citrate.

Immunoelectron microscopy (IEM) of cell cultures. For TF staining of cells, PHMs cultured in 6-well plates were incubated with dilutions (1:100) of an anti-TF murine monoclonal antibody against human TF (American Diagnostica) or an isotype-identical irrelevant murine antibody. PHMs were incubated with

primary antibodies for 2 h, washed with Tris-buffered saline (TBS), and then incubated with dilutions (1:25) of a goat anti–mouse IgG conjugated to 10 nm of colloidal gold (Ted Pella) for 1 h. Cultures were washed in TBS, fixed in 2% glutaraldehyde in 0.1 mol/L phosphate buffer for 1 h, washed, postfixed in 1% osmium tetroxide, and processed for embedment in Poly/Bed 812 resin (Polysciences), as described above.

IEM of culture fluids and plasma. For TF staining of microparticles (MPs) in culture fluids or plasma, 1.5-mL aliquots of culture fluid or 0.5-mL aliquots of plasma were centrifuged at 16,000 *g* for 20 min. Pellets from culture fluid were resuspended in 50 μL of PBS, whereas pellets from plasma were recentrifuged in PBS (0.5 mL) and resuspended in 200 μL of PBS. Drops (5–10 μL) of the suspensions were applied to 300-mesh nickel TEM grids precoated with Formvar and carbon. Grids were immersed for 1 h in dilutions (1:100) of a murine monoclonal antibody against human TF (American Diagnostica) or in an isotype-identical irrelevant murine antibody in TBS containing 0.1% bovine serum albumin and 0.05% Tween-20. Grids were washed and transferred for 1 h to goat anti–mouse IgG labeled with 10-nm gold spheres (Ted Pella) diluted 1:25 in TBS. Grids were then washed by successive immersion in drops of TBS and PBS and were fixed in drops of 2% glutaraldehyde for 1 h. After rinsing in drops of PBS, grids were postfixed in drops of 1% osmium tetroxide, washed in distilled water, and negatively stained with 1% uranyl acetate.

Flow cytometric analysis. MPs were collected from plasma samples, as described above, resuspended in PBS containing a murine anti–TF antibody (American Diagnostica) or an isotype control, and incubated for 30 min. Samples were concentrated, washed in PBS, resuspended in PBS containing goat anti–mouse fluorescein isothiocyanate for 30 min, reconcentrated, rinsed in PBS, and resuspended in 500 μL of PBS. Samples were analyzed in a FACScan flow cytometer with CellQuest software (both from Becton Dickinson).

Immunofluorescence. Formalin-fixed tissue sections were deparafinized and rehydrated, as described elsewhere [29]. Slides were placed in normal goat serum for 30 min, transferred to an anti–TF murine antibody (American Diagnostica), incubated overnight at 4°C, rinsed, incubated in goat anti–mouse alexa 594 (Molecular Probes) for 30 min, rinsed, and mounted in aqueous mounting medium containing 4′,6′-diamidino-2-phenylindole (DAPI; Vector Laboratories). The specificity of the anti–TF antibody for TF in formalin-fixed, paraffin-embedded tissues has been shown in other studies [30]. Cytospins or coverslips were rehydrated, rinsed in PBS, placed in normal goat serum for 30 min, transferred to the anti–TF antibody (American Diagnostica) or an EBOV antibody pool [26] for 1.5 h, incubated in goat anti–mouse alexa 594 (Molecular Probes) for 30 min, rinsed, and mounted in aqueous mounting medium containing DAPI. Negative controls included substitution of isotype-identical irrelevant murine antibodies for the anti-TF antibody and application of the anti-TF antibody to mock-infected cells and uninfected tissues.

RNAse protection assays. PBMCs were separated from EDTA-treated peripheral blood collected from macaques before and after exposure to EBOV [29]. Custom Probe sets were obtained from Pharmingen. The Multiprobe RNAse Protection Assay was performed according to manufacturer's directions (Pharmingen), with minor modifications [29].

RESULTS

Development of coagulation abnormalities. To evaluate the role of the natural anticoagulant systems in the development of DIC during EBOV HF, we assessed several fibrinolytic pathways by use of plasma and/or serum samples temporally obtained from EBOV-infected macaques. Because the amount of available test material was limited, we focused our efforts on the most definitive assays, which had been validated in nonhuman primates and could readily be performed under biosafety level 4 containment. As an example of assay utility, preliminary studies showed that available assays for plasminogen activator inhibitor 1 were not compatible with cynomolgus or rhesus macaques.

Our most striking finding was the rapid decrease in plasma levels of protein C (figure 1*A*), which occurred early during the course of disease and was evident in all macaques at day 2 after infection, and beyond. At days 2 and 3, levels decreased by >40% (2/4 macaques each day) versus preinfection levels. By days 4 and 5, levels decreased by >50% (3/4 macaques each day) versus preinfection values. Plasma levels of protein C rebounded at day 6, but only to 60% of preinfection levels (2/2 macaques). Levels of tPA increased sharply between days 3 and 4, from no detectable difference versus preinfection levels at day 3 to an ~5.5-fold increase over preinfection levels at day 4; this elevation continued to increase through days 5 and 6 (14- and 18-fold over preinfection levels, respectively) (figure 1*B*). Levels of uPA increased in a similar manner, with elevations of ~2-fold over preinfection levels on day 4, 4.5 fold-over preinfection levels on day 5, and nearly 8-fold over preinfection levels on day 6 (statistical significance was observed by day 4; $P < .05$). Levels of FVIIa decreased in most macaques during the course of disease, beginning with a >2-fold decrease at days 1 and 2 (2/3 and 3/4 macaques each day) and increasing to a >3-fold decrease by days 5 and 6 (2/4 and 2/2 macaques each day) (statistical significance was observed by day 5; $P < .05$). Development of fibrin-degradation products (D-dimers) showed rapid increases of 45-fold by day 4 and 55-fold by day 5 (figure 1*C*). Also of relevance in this study, thrombocytopenia developed as platelet counts decreased, from a preinfection mean of 412×10^3 cells/mm^3 to 154×10^3 cells/mm^3 on day 6 (figure 1*D*).

Evidence of fibrin in tissues: association with viral antigen. To further characterize the development of coagulation abnormalities during EBOV infections, the formation of fibrin deposition was analyzed longitudinally, by TEM and by histologic demonstration of polymerized fibrin, in tissue samples from EBOV-infected macaques. TEM performed at day 2 after infection showed rare deposits of fibrin in association with activated (increase in size of nucleus, numbers of lysosomes, and cytoplasmic flaps) tissue macrophages in the splenic marginal zone (1/3 macaques). By day 3, small focal deposits of fibrin were associated with activated tissue macrophages in red pulp and the marginal zone (2/4 macaques). PTAH-positive fibrin was evident by day 4; multifocal deposits were present in the sinusoids and marginal zones of spleen (figure 2*A*) and were less frequently observed in the cords of Bilroth (3/4 macaques). Fibrin was occasionally observed in hepatic sinusoids, usually closely associated with Kupffer cells (3/4 macaques), and multiple foci of PTAH-positive fibrin were detected in blood vessels of the renal medulla (2/4 macaques) (figure 2*B*). By day 5, the presence of fibrin deposits dramatically increased. Fibrin thrombi and fibrinocellular thrombi, composed of monocytes enmeshed in fibrin, were focally identified in vessels of most tissues evaluated. PTAH-positive fibrin was occasionally seen in hepatic sinusoids, usually closely associated with Kupffer cells (4/4 macaques); was frequently present in red pulp sinusoids, marginal zones of spleen, and the cords of Bilroth (4/4 macaques); and was especially prominent in blood vessels of the renal medulla (4/4 macaques). TEM findings at day 5 were similar. A high proportion of hepatic sinusoids were filled with fibrin deposits, fibrinocellular debris, and free virions. Deposits of fibrin and fibrinocellular debris in spleen were so heavy and widespread that normal architecture was almost completely lost (4/4 macaques); there was a strong demarcation of venous sinuses by fibrin deposits between the basement membrane and the cords of Bilroth. Macaques evaluated on day 6 showed similar patterns of splenic fibrin deposition, but with more abundant fibrin, and PTAH-positive fibrin thrombi were also present in pulmonary vessels (2/3 macaques) and renal glomeruli (1/3 macaques).

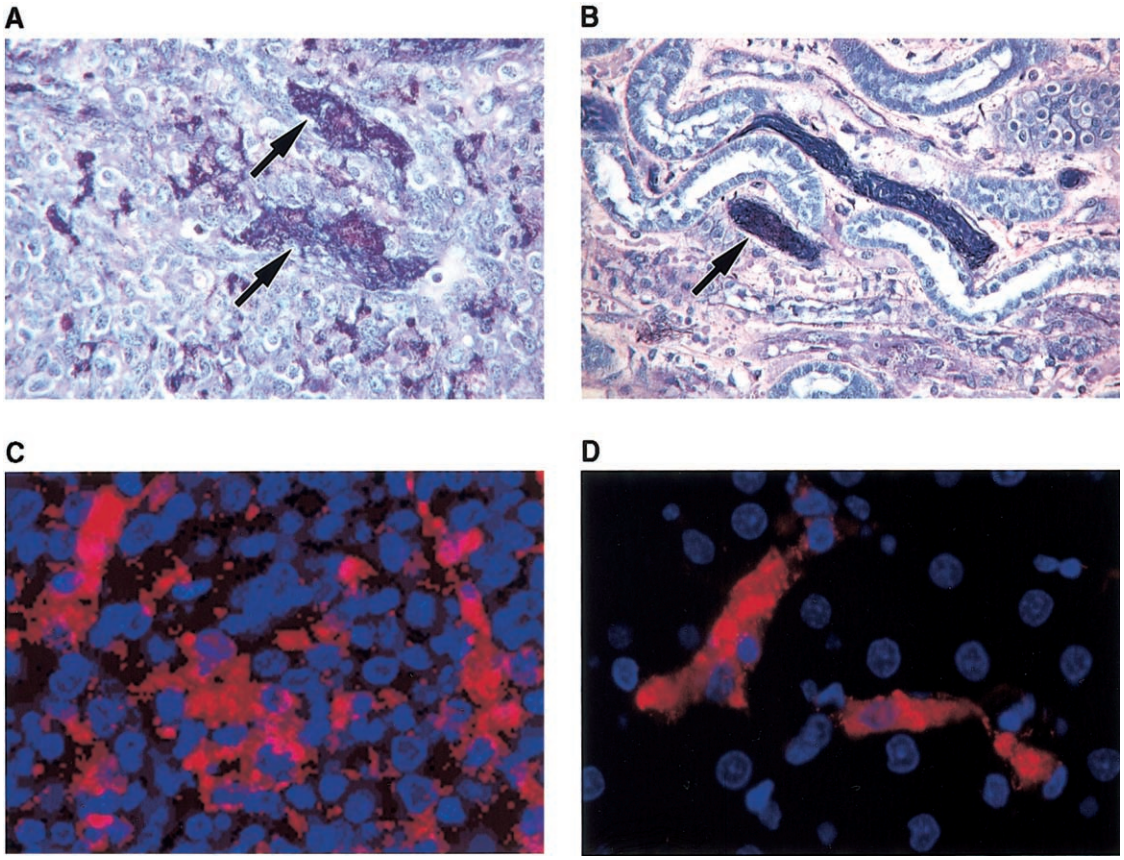

Figure 2. Development of fibrin and association with Ebola virus (EBOV) antigen. *A,* Phosphotungstic acid hematoxylin (PTAH)–positive fibrin *(arrows)* in the marginal zone of the spleen of a cynomolgus macaque at day 4 after infection. *B,* PTAH-positive fibrin *(arrows)* in blood vessels of renal medulla of a cynomolgus macaque at day 4. *C,* Indirect fluorescent antibody analysis (IFA) showing abundance of EBOV-positive cells in the spleen of a cynomolgus macaque at day 4. *D,* IFA showing EBOV antigen in Kupffer cells and hepatic sinusoids of a cynomolgus macaque at day 4; identification of Kupffer cells was confirmed by electron microscopy (data not shown).

It is noteworthy that the presence of fibrin appeared to be closely associated with the presence of EBOV-infected cells. For example, PTAH staining did not show deposition of fibrin in the liver until day 4, the time when infected cells were readily detected by indirect fluorescent antibody analysis (IFA) (figure 2*C* and 2*D*). Likewise, the abundance of fibrin paralleled the level of EBOV antigen detected. Organ infectivity titers corroborated these findings. Specifically, by day 3 after infection, 2 of 4 macaques had infectious virus in the liver (virus titer [mean ± SD, here and below], 2.40 ± 2.77 $\log_{10}$ pfu/g of tissue); by day 4, infectious virus was detected in livers of all 4 macaques (virus titer, 6.89 ± 1.01 $\log_{10}$ pfu/g of tissue). By day 2, infectious virus was detected in the spleen of 1 of 3 macaques (virus titer, 1.08 ± 1.87 $\log_{10}$ pfu/g of tissue); interestingly, the single macaque with infectious virus in the spleen was also the only macaque evaluated at day 2 with fibrin detected by TEM. By day 3, all macaques had infectious virus detected in their spleens (virus titer, 4.88 ± 0.43 $\log_{10}$ pfu/g of tissue); by day 4, the virus titer was 6.91 ± 1.03 $\log_{10}$ pfu/g of tissue.

TEM also demonstrated a close association between fibrin deposits and EBOV-infected cells. The most remarkable TEM observation at day 4 was the appearance of fibrin mesh networks that completely encased many EBOV-infected lymphoid tissue macrophages (figure 3*A*), particularly in the subcapsular sinuses of inguinal lymph nodes (2/4 macaques). These fibrin mesh networks were also detected by TEM around EBOV-infected Kupffer cells and cells with morphology consistent with dendritic cells (DCs) or fibroblastic reticular cells. This fibrin encapsulation was observed only in cells with characteristic EBOV intracellular inclusion material and/or budding virions and proliferated membranes [31]; neighboring cells (neutrophils, lymphocytes, red blood cells, and macrophages) that did not exhibit morphological evidence of EBOV infection were not associated with these fibrin mesh networks (figure 3*B*).

Expression of TF mRNA and protein in PBMCs in vivo. To explore the potential role of TF in inducing the coagulation cascade during EBOV infection, PBMCs were collected from EBOV-infected macaques, and mRNA transcripts were analyzed. Increased TF transcripts were observed in 3 of 4 macaques by day 3 after infection and in all macaques from day 4 and beyond (figure 4*A*). IFA for TF was also performed on cytospins prepared from available blood samples. IFA confirmed expression of TF and showed increased numbers of TF-positive cells during the course of the infection (figure 4*B* and 4*C*).

Expression of TF protein in tissues. Immunohistochemical analysis was performed on liver and spleen tissue from EBOV-infected macaques. Early-stage tissues, obtained at days 1 and 2, were compared with those obtained at mid-to-late stages of infection (days 4 and 5). Although antigen retrieval for TF proved to be problematic in tissues that had been stored in formalin for 4 weeks, clear increases in the number of cells expressing TF, particularly splenic macrophages, were seen at days 4 and 5. In addition to macrophages, other cells positive for TF antigen included polymorphonuclear neutrophils (PMNs) and endothelial cells. Interestingly, expression of TF in endothelial cells appeared to be focal and was not uniform (e.g., occasional vessels displayed intense staining, whereas many others showed mild-to-no staining). Circulating TF-positive cells were also ob-

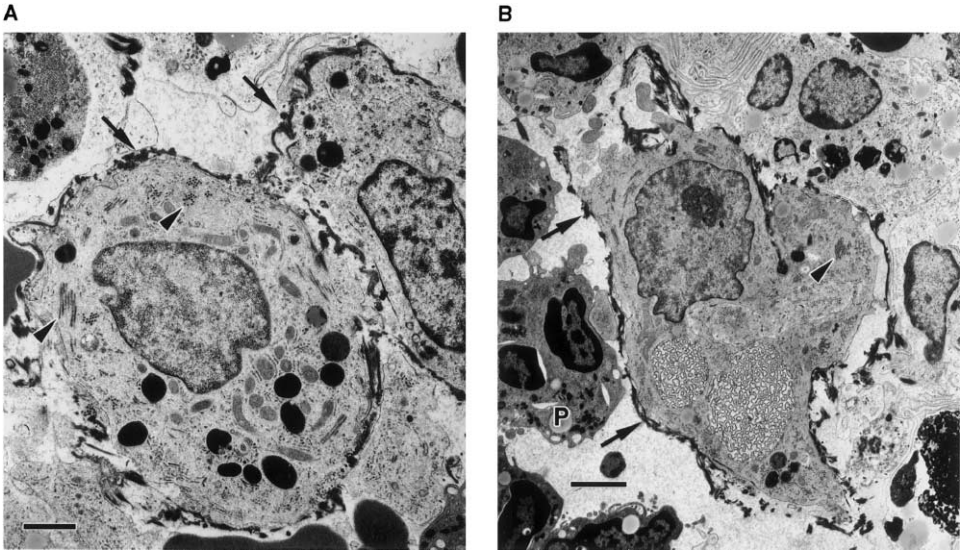

Figure 3. Association of fibrin with Ebola virus (EBOV)–infected cells, as detected by transmission electron microscopy. *A,* Encasement of EBOV-infected tissue macrophages with fibrin in subcapsular sinus of inguinal lymph node of a cynomolgus macaque at day 4 after infection. *Bar,* 1.5 μm. *B,* Fibrin encapsulation of EBOV-infected tissue macrophage in the same area of a different macaque at day 5. Note that adjacent polymorphonuclear neutrophils (P) show no association with fibrin. *Bar,* 2.5 μm. *Arrowheads,* EBOV inclusion material; *arrows,* fibrin.

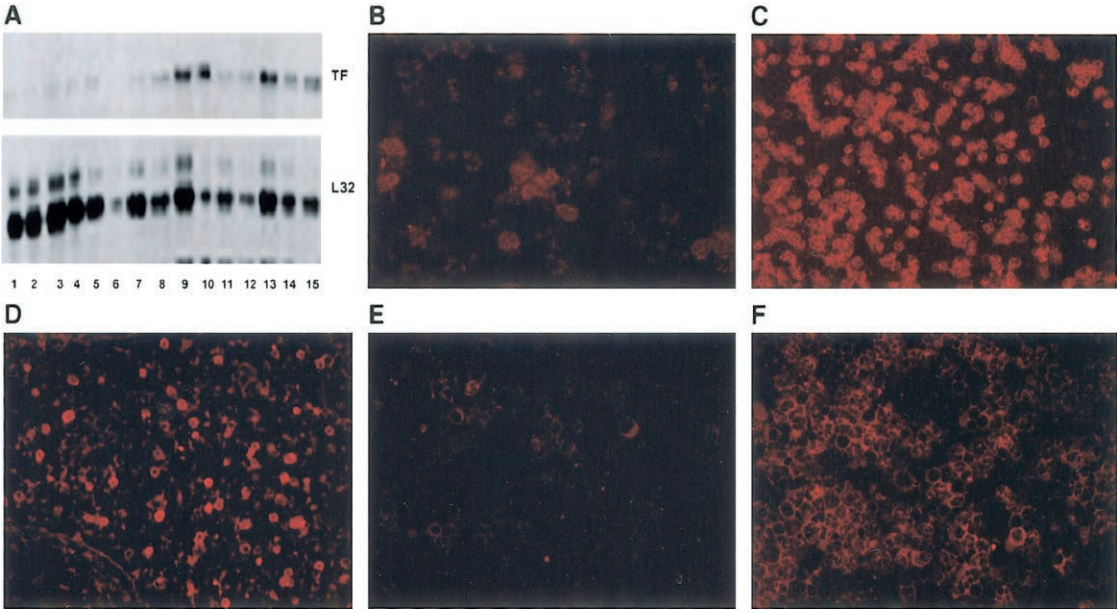

Figure 4. Expression of tissue factor (TF) mRNA and protein in vivo. *A,* Analysis of TF mRNA production in peripheral blood mononuclear cells (PBMCs) of Ebola virus (EBOV)–infected macaques. Representative RNase protection assay comparing 3 different macaques before infection *(lanes 1–3),* and 2 macaques/day at days 1 *(lanes 4* and *5),* 2 *(lanes 6* and *7),* 3 *(lanes 8* and *9),* 4 *(lanes 10* and *11),* 5 *(lanes 12* and *13),* and 6 *(lanes 14* and *15)* after infection. The control L32 ribosomal gene, contained in the Riboprobe template set, was used to indicate relative loading of the different lanes. Indirect fluorescent antibody analysis (IFA) was performed for TF of cytospins prepared from PBMCs of an EBOV-infected rhesus macaque at day 2 *(B)* and at day 5 *(C)* after infection. *D,* IFA for TF showing TF-positive circulating cells in large hepatic vessel of a cynomolgus macaque at day 5. *E,* IFA for TF of cytospins prepared from the spleen of an EBOV-infected cynomolgus macaque at day 3 and at day 5 *(F).*

served in larger vessels (figure 4*D*). To confirm these findings, and to circumvent problems associated with storing tissues in formalin for extended periods of time, cytospins were prepared from dissociated spleens of available EBOV-infected macaques. IFA for TF on these samples confirmed increasing numbers of TF-positive cells during the disease course (figure 4*E* and 4*F*).

Production of membrane MPs in vivo. Membrane MPs are shed from the plasma membrane of most eukaryotic cells undergoing activation or apoptosis [32–34]. To test the hypothesis that TF-expressing MPs are formed during EBOV infection, flow cytometry and IEM were performed on a cohort of plasma samples from EBOV-infected macaques. Flow cytometry demonstrated the development of a TF-positive MP population (figure 5*A*). IEM analysis of these samples confirmed that the MPs were fragments of cell membranes, of a variety of sizes (range, 0.1–1.0 μmol/L) and conformations, and that the labeling of TF on these MPs was very specific (figure 5*B* and 5*C*). TF-positive MPs were infrequently seen at day 1 (<1 TF-positive MP/field of 300 electron microscopy grid), but, by days 4 and 5, gold sphere–labeled MPs were readily detected in plasma of all macaques analyzed (>40 TF-positive MPs/field). In addition, the intensity of gold-sphere labeling of MP increased during the infection (e.g., at day 1, only 3–4 gold spheres were seen on MPs, whereas >10 gold spheres were usually seen on MPs by day 4).

Expression of TF mRNA and protein in vitro. To confirm expression of TF in mononuclear phagocytes, cultures of PHMs were established from 3 separate donors and infected with EBOV. Primary human endothelial cells, macrovascular HUVECs, and microvascular HMVEC-Ls were used for comparative purposes. Analysis of PHM and endothelial-cell gene response showed increased TF transcripts in PHMs as early as 1 h after infection (figure 6*A*); increased levels of TF transcripts were also seen in PHMs at 24 and 48 h. Increased levels of TF transcripts were not detected in HUVECs or HMVEC-Ls (data not shown), even though EBOV replicated in these cells, as evidenced by viral infectivity titration, which showed ~6 $\log_{10}$ pfu/mL of infectious EBOV in culture fluid. IFA confirmed TF protein expression in PHMs at 48 h (figure 6*B–D*). IEM also corroborated expression of TF and revealed that TF was primarily localized to PHM showing morphological evidence of EBOV infection [31]. TF-positive gold-sphere labeling was seen only rarely in PHMs that showed no morphologic evidence of infection. In many cases, TF was colocalized with areas of EBOV-induced proliferated membranes [31] (figure 6*E* and 6*F*). Occasional foci of TF were localized to nondescript areas along and just beneath the plasma membrane. Analysis of fluids from PHM cultures by IEM showed TF-positive MPs ranging in size from 0.1 μmol/L to nearly 1.0 μmol/L (figure 6*G*). Some of these MPs had attached viral particles and were interpreted to be portions of the EBOV-induced proliferated membranes

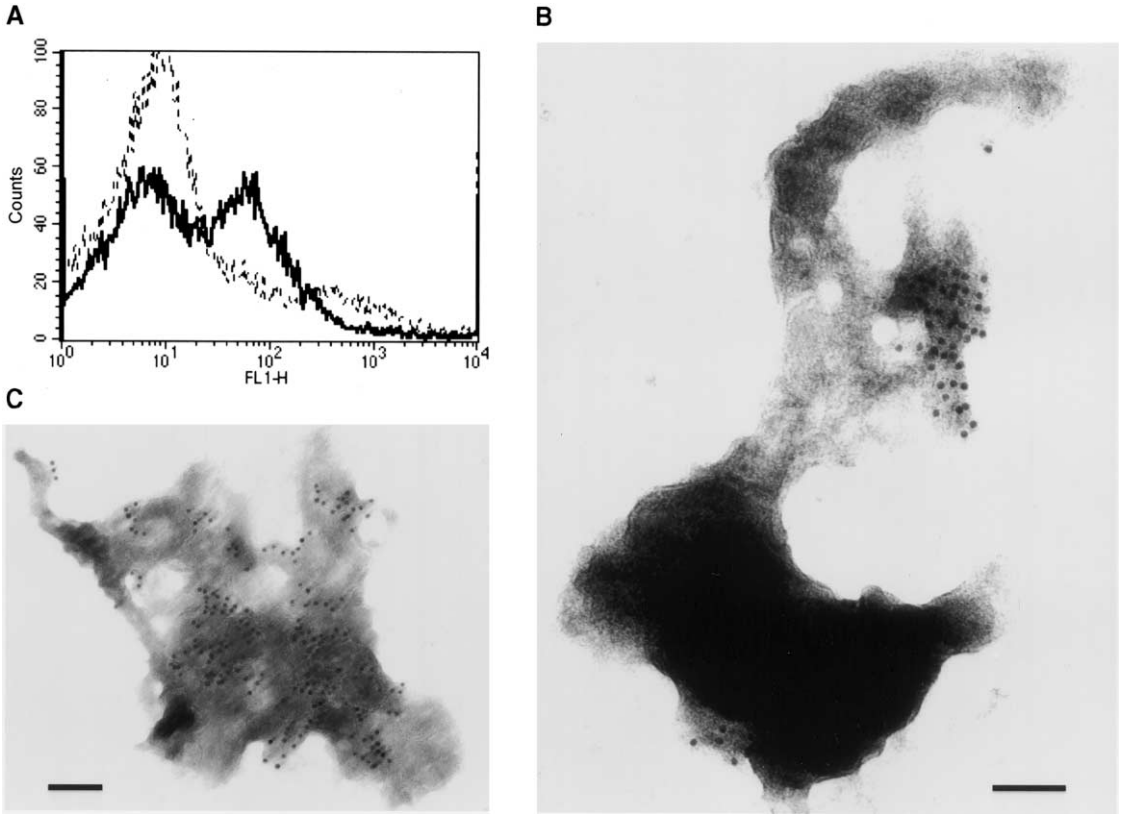

Figure 5. Detection of membrane microparticles (MPs) in vivo. *A,* Flow cytometric analysis showing development of a distinct population of tissue factor (TF)–positive MPs during Ebola virus (EBOV) infection of cynomolgus macaques. *Dashed line,* MPs obtained from plasma of a macaque at day 1 after infection; *solid line,* MPs obtained from plasma of a macaque at day 5. Results for MPs obtained from preinfection plasma (data not shown) were consistent with MPs obtained at day 1 after infection. *B,* Immunoelectron microscopy (IEM) showing specific gold-sphere labeling for TF of MPs isolated from plasma of an EBOV-infected rhesus macaque at day 9. *Bar,* 100 nm. *C,* IEM showing intense gold-sphere labeling for TF of MPs isolated from plasma of an EBOV-infected cynomolgus macaque at day 4. *Bar,* 100 nm. FL1-H, forward light scatter.

seen in thin sections of EBOV-infected PHMs. It is noteworthy that the EBOV virions did not express TF, yet the attached membranes were TF positive by IEM.

DISCUSSION

The development of DIC is a characteristic clinical manifestation of EBOV infection in primates; however, the mechanisms that trigger coagulation abnormalities remain unknown. The present study provides the first insight into the pathogenesis of coagulation system dysregulation and suggests that the development of coagulation abnormalities may occur much earlier than previously thought. Although it is likely that the coagulopathy seen in EBOV HF is caused by multiple factors, particularly during the later stages of disease, the data presented here strongly implicate TF expression/release from EBOV-infected monocytes/macrophages as a key factor that induces the development of coagulation irregularities seen in EBOV infections.

DIC is not a primary disorder but is a complication of an underlying disease, usually an infection, that triggers a massive activation of the clotting cascade. The major initiating factor is the release or expression of TF in response to endotoxins, various cytokines, or other cellular factors [6]. For example, in the case of dengue HF, Wills et al. [35] postulated that dengue infection may activate fibrinolysis by degrading fibrinogen directly, thus promoting secondary activation of procoagulant homeostatic mechanisms that include increases in plasma levels of TF. Here, we show that expression of TF was observed only in monocytes/macrophages with morphological evidence of EBOV replication, suggesting that expression of TF may be directly induced by EBOV infection. Given the large number of EBOV-infected monocyte/macrophages associated with primate infections [3, 25, 26], it is likely that the overproduction of TF is the primary initiating factor for the observed coagulopathy.

In these tissues, the appearance of fibrin deposits, coinciding with detectable viremia and infectious virus, strongly supports a direct link with viral infection. The appearance of fibrin mesh networks that selectively encased EBOV-infected lymphoid tissue macrophages and Kupffer cells, by day 4, and DCs, by day 5, not only corroborate this observation but also suggest that

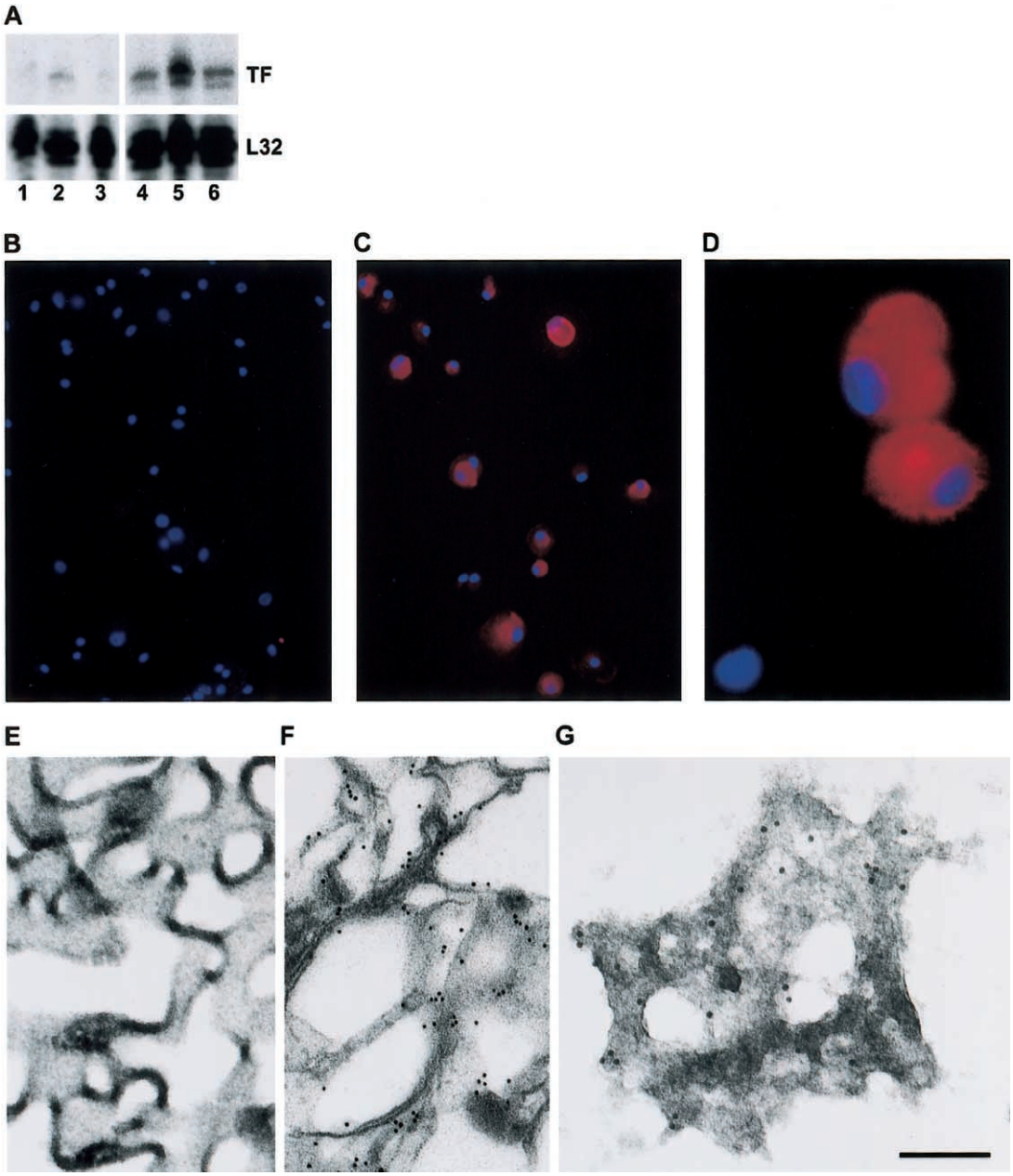

Figure 6. Expression of tissue factor (TF) mRNA and protein in vitro. *A,* Analysis of TF mRNA production in Ebola virus (EBOV)–infected cultures. Representative RNase protection assays are shown, comparing mock-infected primary human monocytes/macrophages (PHMs) at 1, 24, and 48 h (*lanes 1–3,* respectively) and EBOV-infected PHMs at 1, 24, and 48 h (*lanes 4–6,* respectively). *B,* Indirect fluorescent antibody analysis (IFA) for TF from mock-infected PHMs at 48 h after infection. *C,* IFA for TF from EBOV-infected PHMs at 48 h. *D,* High-power view of EBOV-infected PHMs at 48 h (similar to field shown in panel *C*). Preembedment immunoelectron microscopy (IEM) of EBOV-infected PHMs at 48 h after infection incubated with isotype-irrelevant murine antibody *(E),* and incubated with anti-TF antibody showing 10-nm gold-sphere labeling of proliferated membranes *(F). G,* IEM showing gold-sphere labeling for TF of microparticles isolated from culture fluid of EBOV-infected PHMs at 48 h. *Bar,* 150 nm.

viral infection resulted in up-regulation of a protein capable of triggering the coagulation cascade. RNA analysis, IFA, and TEM all show that expression of TF is up-regulated during EBOV infection and likely triggers activation of the coagulation system, producing the marked fibrin encasement of EBOV-infected cells.

Analysis of macaque PBMC mRNA demonstrated increased levels of TF transcripts by day 3; IFA confirmed these findings. Because monocytes/macrophages are the only cells in the blood circulation compartment that express TF on their surface [15, 36] and because differential cell counts show that monocytes represented only 1%–6% of the total white blood cells of any

of the 25 macaques in the present study, it is likely that the level of TF transcripts in monocytes is more marked than that in total PBMCs. Cells morphologically consistent with monocytes/macrophages or PMNs were positive for TF. TEM analysis of macaque tissues demonstrated fibrin formation only around EBOV-infected cells, including lymphoid monocytes/macrophages, Kupffer cells, and DCs. Fibrin formation was not observed around PMNs, which do not support EBOV replication. It is not surprising that PMNs may phagocytose and store TF protein released by monocytes/macrophages, but, unless they are induced to up-regulate mRNA transcripts and express TF protein on the cell surface, PMNs are not likely to trigger the coagulation system. The observation of TF by IFA and the lack of fibrin associated with these cell types by TEM is consistent with this view and also implicates monocytes/macrophages as key sources for TF protein during EBOV infection. Moreover, up-regulation of TF mRNA and protein in EBOV-infected monocytes/macrophages in vitro further corroborates this hypothesis.

Levels of expression of TF may also be affected by the production of various cytokines and chemokines. Proinflammatory cytokines, such as interleukin (IL)–6, have been shown to effectively up-regulate expression of TF on monocytes [37, 38]. In EBOV-infected macaques, increased levels of IL-6 have been reported by day 4 after infection [29]. Splenocyte stimulation with TF also induces the selective release of the monocyte chemoattractant molecule macrophage inflammatory protein (MIP)–1α in vitro [39]. Increased levels of MIP-1α have been demonstrated in EBOV-infected macaques and cultures of infected monocytes/macrophages [29]. Taken together, these findings suggest that expression of TF can be amplified during the later stages of disease when EBOV-infected cells, which selectively express TF, release cytokines/chemokines that may either directly up-regulate levels of TF or attract additional preferred target cells to foci of infection, thereby exacerbating activation of the extrinsic coagulation pathway.

The present study also implicates TF expressed on MPs, which may be generated by EBOV infection of monocytes/macrophages, as playing an important role in disease pathogenesis. We have demonstrated that TF-positive MPs are shed from EBOV-infected monocytes/macrophages in vitro; furthermore, we have shown increased numbers of TF-positive MPs in plasma of EBOV-infected macaques. The procoagulant potential of MPs is supported by clinical studies showing elevated levels of circulating MPs in patients with an increased risk for thromboembolic events (e.g., DIC) [33, 34]. Our observation of MPs during EBOV infection is not unprecedented. Recently, it was reported that patients with fulminant meningococcal sepsis had CD14- and TF-positive MPs and that these MPs also induced extreme thrombin generation in vitro [33].

The present study has suggested that protein C may be a critical component of the observed coagulation dysfunction in EBOV HF. The protein C system is one of the main anticoagulant mechanisms in blood [40]. Growing evidence also suggests that protein C has direct anti-inflammatory properties and modulating activity on cellular functions, likely by blocking NF-κB nuclear translocation [41–43]. The rapid decrease in plasma levels of protein C concomitant with progression of disease was a prominent finding in the present study. Reduced levels of protein C are found in the majority of patients with sepsis and are associated with an increased risk of death [44, 45]. Moreover, protein C deficiency appears to develop well before the onset of defined clinical variables of severe sepsis or septic shock [45, 46] and may be considered a prognostic indicator [47]. Clearly, in this primate model of EBOV, identifying protein C abnormalities (that so closely parallel protein C anomalies in human coagulopathies) offers an ideal target for chemotherapeutic interventions. Administration of activated protein C was protective in a baboon model of lethal *Escherichia coli* sepsis [48]. More recently, treatment with recombinant human activated protein C significantly reduced mortality in patients with severe sepsis [49]; furthermore, biological activity of activated protein C was demonstrated by finding greater decreases in levels of D-dimer and IL-6 in patients who received activated protein C than in those who received placebo.

The selection of an appropriate nonhuman primate model of EBOV HF requires careful consideration of the species, sex, age, route of infection, dose of EBOV administered, and nature of the challenge virus itself. It is very difficult to compare results from the various published studies of EBOV HF in nonhuman primates because of considerable differences among these factors. Species-specific differences in the appearance of coagulopathies were reported in one study. Specifically, fibrin deposition in vessels was associated with EBOV infection of African green monkeys, whereas hemorrhages were a feature associated with EBOV disease in baboons [50]. Consistent with the previous findings shown for African green monkeys [26, 50] and rhesus macaques [3, 4], we observed fibrin in vessels of the macaques used in the present study. Although the present study primarily focused on cynomolgus macaques, we did not see species-specific differences in coagulopathy among the cynomolgus macaques and a small number of rhesus macaques that were primarily used as a pilot group to detect any clear species-specific differences.

Identifying TF as an initiating aspect of DIC and dysregulation of protein C as a potentially exacerbating factor may be central to explaining the mechanisms that trigger the hemorrhagic diathesis of EBOV infection. The present study represents a first step in demonstrating that chemotherapeutic strategies aimed at controlling TF overexpression and dysregulation of the protein C system may ameliorate the effects of EBOV HF. Strategies that have proven to be successful for treating patients with similar clinical pictures, such as administering

activated protein C to patients with severe sepsis, may also have utility in treating EBOV infections. It is also likely that combination therapy with multiple coagulation-modulating agents may ultimately prove to be the best approach for treating the inherent DIC. Rodent models of EBOV HF do not exhibit the hemorrhagic manifestations that characterize primate EBOV infections [4, 27], which may explain the failure of rodents to predict antiviral drug efficacy in primates [4, 28, 51]. The present study has suggested that antiviral strategies shown to control EBOV replication in rodents may be significantly improved by effective management of coagulopathy in primates.

Acknowledgments

We thank Denise Braun, Joan Geisbert, Lynda Miller, Roswita Moxley, Jeff Brubaker, Steve Moon, Neil Davis, and Larry Ostby, for their expert technical assistance; Michael Hensley, Brad Stiles, and Doug Reed, for helpful discussions and comments; and Tom Larsen, for skillful assistance with necropsies.

References

1. Sanchez A, Khan AS, Zaki SR, Nabel GJ, Ksiazek TG, Peters CJ. Filoviridae. In: Knipe DM, Howley PM, eds. Fields virology. Philadelphia: Lippincott, Williams, & Wilkins, **2001**:1279–304.
2. Fisher-Hoch SP, Brammer LT, Trappier SG, et al. Pathogenic potential of filoviruses: role of geographic origin of primate host and virus strain. J Infect Dis **1992**; 166:753–63.
3. Jaax NK, Davis KJ, Geisbert TW, et al. Lethal experimental infection of rhesus monkeys with Ebola-Zaire (Mayinga) virus by the oral and conjunctival route of exposure. Arch Pathol Lab Med **1996**; 120:140–55.
4. Geisbert TW, Pushko P, Anderson K, Smith J, Davis KJ, Jahrling PB. Evaluation in nonhuman primates of vaccines against Ebola virus. Emerg Infect Dis **2002**; 8:503–7.
5. Levi M, de Jonge E, van der Poll T, ten Cate H. Disseminated intravascular coagulation. Thromb Haemost **1999**; 82:695–705.
6. Mammen EF. Disseminated intravascular coagulation (DIC). Clin Lab Sci **2000**; 13:239–45.
7. Levi M. Pathogenesis and treatment of disseminated intravascular coagulation in the septic patient. J Crit Care **2001**; 16:167–77.
8. Gando S, Nanzaki S, Kemmotsu O. Disseminated intravascular coagulation and sustained systemic inflammatory response syndrome predict organ dysfunctions after trauma: application of clinical decision analysis. Ann Surg **1999**; 229:121–7.
9. Levi M, de Jonge E, van der Poll T, ten Cate H. Advances in the understanding of the pathogenetic pathways of disseminated intravascular coagulation result in more insight in the clinical picture and better management strategies. Semin Thromb Hemost **2001**; 27:569–75.
10. Wilson RF, Mammen EF, Tyburski JG, Warsow KM, Kubinec SM. Antithrombin levels related to infections and outcome. J Trauma **1996**; 40: 384–7.
11. Taylor FB Jr, Chang A, Ruf W, et al. Lethal *E. coli* septic shock is prevented by blocking tissue factor with monoclonal antibody. Circ Shock **1991**; 33:127–34.
12. Arai A, Hirano H, Ueta Y, Hamada T, Mita T, Shirahata A. Detection of mononuclear cells as the source of the increased tissue factor mRNA in the liver from lipopolysaccharide-treated rats. Thromb Res **2000**; 97:153–62.
13. Drake TA, Cheng J, Chang A, Taylor FB Jr. Expression of tissue factor, thrombomodulin, and E-selectin in baboons with lethal *Escherichia coli* sepsis. Am J Pathol **1993**; 142:1458–70.
14. Osterud B, Bjorklid E. The tissue factor pathway in disseminated intravascular coagulation. Semin Thromb Hemost **2001**; 27:605–17.
15. Tremoli E, Camera M, Toschi V, Colli S. Tissue factor in atherosclerosis. Atherosclerosis **1999**; 144:273–83.
16. Hara S, Asada Y, Hatakeyama K, et al. Expression of tissue factor and tissue factor pathway inhibitor in rat lungs with lipopolysaccharide-induced disseminated intravascular coagulation. Lab Invest **1997**; 77: 581–9.
17. Gedigk P, Bechtelsheimer H, Korb G. Die pathologische anatomie der Marburg-virus-Krankheit. Dtsch Med Wochenschr **1968**; 93:590–601.
18. Murphy FA. Pathology of Ebola virus infection. In: Pattyn SR, ed. Ebola virus haemorrhagic fever. New York: Elsevier/North-Holland Biomedical Press, **1978**:43–60.
19. Geisbert TW, Jaax NK. Marburg hemorrhagic fever: report of a case studied by immunohistochemistry and electron microscopy. Ultrastruct Pathol **1998**; 22:3–17.
20. Egbring R, Slenczka W, Baltzer G. Clinical manifestations and mechanism of the hemorrhagic diathesis in Marburg virus disease. In: Martini GA, Siegert R, eds. Marburg virus disease. New York: Springer-Verlag, **1971**:41–9.
21. Gear JS, Cassel GA, Gear AJ, et al. Outbreak of Marburg virus disease in Johannesburg. BMJ **1975**; 4:489–93.
22. Isaacson M, Sureau P, Courteille G, Pattyn SR. Clinical aspects of Ebola virus disease at the Ngaliema Hospital, Kinshasa, Zaire, 1976. In: Pattyn SR, ed. Ebola virus haemorrhagic fever. New York: Elsevier/North-Holland Biomedical Press, **1978**:15–20.
23. World Health Organization. Ebola haemorrhagic fever in Zaire, 1976: report of an international commission. Bull World Health Organ **1978**;56: 271–93.
24. Fisher-Hoch SP, Platt GS, Neild GH, et al. Pathophysiology of shock and hemorrhage in a fulminating viral infection (Ebola). J Infect Dis **1985**; 152:887–94.
25. Geisbert TW, Jahrling PB, Hanes MA, Zack PM. Association of Ebola related Reston virus particles and antigen with tissue lesions of monkeys imported to the United States. J Comp Pathol **1992**; 106:137–52.
26. Davis KJ, Anderson AO, Geisbert TW, et al. Pathology of experimental Ebola virus infection in African green monkeys. Arch Pathol Lab Med **1997**; 121:805–19.
27. Bray M, Hatfill S, Hensley L, Huggins JW. Haematological, biochemical and coagulation changes in mice, guinea-pigs and monkeys infected with a mouse-adapted variant of Ebola Zaire virus. J Comp Pathol **2001**; 125: 243–53.
28. Jahrling PB, Geisbert TW, Geisbert JB, et al. Evaluation of immune globulin and recombinant interferon-α2b for treatment of experimental Ebola virus infections. J Infect Dis **1999**; 179(Suppl 1):S224–34.
29. Hensley LE, Young HA, Jahrling PB, Geisbert TW. Proinflammatory response during Ebola virus infection of primate models: possible involvement of the tumor necrosis factor receptor superfamily. Immunol Lett **2002**; 80:169–79.
30. Grossniklaus HE, Ling JX, Wallace TM, et al. Macrophage and retinal epithelium expression of angiogenic cytokines in choroidal neovascularization. Mol Vis **2002**; 8:119–26.
31. Geisbert TW, Jahrling PB. Differentiation of filoviruses by electron microscopy. Virus Res **1995**; 39:129–50.
32. Mesri M, Altieri DC. Endothelial cell activation by leukocyte microparticles. J Immunol **1998**; 161:4382–7.
33. Nieuwland R, Berckmans RJ, McGregor S, et al. Cellular origin and procoagulant properties of microparticles in meningococcal sepsis. Blood **2000**; 95:930–5.
34. Sabatier F, Roux V, Anfosso F, Camoin L, Sampol J, Dignat-George F. Interaction of endothelial microparticles with monocytic cells in vitro induces tissue factor–dependent procoagulant activity. Blood **2002**; 99: 3962–70.
35. Wills BA, Oragui EE, Stephens AC, et al. Coagulation abnormalities

in dengue hemorrhagic fever: serial investigations in 167 Vietnamese children with dengue shock syndrome. Clin Infect Dis **2002**; 35:277–85.
36. Giesen PL, Rauch U, Bohrmann B, et al. Blood-borne tissue factor: another view of thrombosis. Proc Natl Acad Sci USA **1999**; 96:2311–5.
37. Neumann F-J, Ott I, Marx N, et al. Effect of human recombinant interleukin-6 and interleukin-8 on monocyte procoagulant activity. Arterioscler Thromb Vasc Biol **1997**; 17:3399–405.
38. Grignani G, Maiolo A. Cytokines and hemostasis. Haematologica **2000**; 85:967–72.
39. Bokarewa MI, Morissey JH, Tarkowski A. Tissue factor as a proinflammatory agent. Arthritis Res **2002**; 4:190–5.
40. Esmon CT. Regulation of blood coagulation. Biochim Biophys Acta **2000**; 1477:349–60.
41. Yan SB, Grinnell BW. Antithrombotic and anti-inflammatory agents of the protein C anticoagulant pathway. Ann Rep Med Chem **1994**; 11:103–12.
42. Murakami K, Okajima K, Uchiba M, et al. Activated protein C prevents LPS-induced pulmonary vascular injury by inhibiting cytokine production. Am J Physiol **1997**; 272:L197–202.
43. Esmon CT. Protein C anticoagulant pathway and its role in controlling microvascular thrombosis and inflammation. Crit Care Med **2001**; 29: S48–52.
44. Fourrier F, Chopin C, Goudemand J, et al. Septic shock, multiple organ failure, and disseminated intravascular coagulation: compared patterns of antithrombin III, protein C, and protein S deficiencies. Chest **1992**; 101:816–23.
45. Lorente JA, Garcia-Frade LJ, Landin L, et al. Time course of hemostatic abnormalities in sepsis and its relation to outcome. Chest **1993**; 103: 1536–42.
46. Kidokoro A, Iba T, Fukunaga M, Yagi Y. Alterations in coagulation and fibrinolysis during sepsis. Shock **1996**; 5:223–8.
47. Fisher CJ, Yan B. Protein C levels as a prognostic indicator of outcome in sepsis and related diseases. Crit Care Med **2000**; 28:S49–56.
48. Taylor FB Jr, Chang A, Esmon CT, D'Angelo A, Vigano-D'Angelo S, Blick KE. Protein C prevents the coagulopathic and lethal effects of *Escherichia coli* infusion in the baboon. J Clin Invest **1987**; 79:918–25.
49. Bernard GR, Vincent JL, Laterre PF, et al. Efficacy and safety of recombinant human activated protein C for severe sepsis. N Engl J Med **2001**; 344:699–709.
50. Ryabchikova EI, Kolesnikova LV, Luchko SV. An analysis of features of pathogenesis in two animal models of Ebola virus infection. J Infect Dis **1999**; 179(Suppl 1):S199–202.
51. Huggins JW, Zhang ZX, Davis K, Coulombe RA. Inhibition of Ebola virus by S-adenosylhomocysteine hydrolase inhibitors. Antiviral Res **1995**; 26:A301.